



Published in final edited form as:

Science. 2013 March 15; 339(6125): 1328–1331. doi:10.1126/science.1230593.

Proteomic Mapping of Mitochondria in Living Cells via Spatially-Restricted Enzymatic Tagging

Hyun-Woo Rhee^{#1,‡}, Peng Zou^{#1}, Namrata D. Udeshi², Jeffrey D. Martell¹, Vamsi K. Mootha^{2,3}, Steven A. Carr², and Alice Y. Ting^{1,2,*}

¹Department of Chemistry, Massachusetts Institute of Technology, Cambridge, MA 02139, USA

²Broad Institute of MIT and Harvard, Cambridge, MA 02142, USA

³Department of Molecular Biology, Massachusetts General Hospital, and Department of Systems Biology, Harvard Medical School, Boston, MA 02115, USA

[#] These authors contributed equally to this work.

Abstract

Microscopy and mass spectrometry (MS) are complementary techniques: the former provides spatiotemporal information in living cells, but only for a handful of recombinant proteins, while the latter can detect thousands of endogenous proteins simultaneously, but only in lysed samples. Here we introduce technology that combines these strengths by offering spatially- and temporally-resolved proteomic maps of endogenous proteins within living cells. The method relies on a genetically-targetable peroxidase enzyme that biotinylates nearby proteins, which are subsequently purified and identified by MS. We used this approach to identify 495 proteins within the human mitochondrial matrix, including 31 not previously linked to mitochondria. The labeling was exceptionally specific and distinguished between inner membrane proteins facing the matrix versus the intermembrane space (IMS). Several proteins previously thought to reside in the IMS or outer membrane, including protoporphyrinogen oxidase, were reassigned to the matrix. The specificity of live-cell peroxidase-mediated proteomic mapping combined with its ease of use offers biologists a powerful tool for understanding the molecular composition of living cells.

We sought to develop a method that circumvents the limited specificity and loss of material associated with organelle purification in traditional MS proteomics. Our approach was to tag the proteome of interest with a chemical handle such as biotin while the cell was still alive, with all membranes, complexes, and spatial relationships preserved. We thus required a genetically targetable labeling enzyme that covalently tags its neighbors, but not more distant proteins, in living cells. One candidate is promiscuous biotin ligase (1–3), but its labeling kinetics are extremely slow (requiring 24 hours (1, 2); Fig. S1), and the proposed mechanism proceeds through a biotin-adenylate ester, which has a half-life of minutes, implying a large labeling radius. Horseradish peroxidase (HRP)-catalyzed nitrene generation is another possibility (4), but we were unable to detect this labeling (Fig. S2), and HRP is inactive when expressed in the mammalian cytosol (5).

*To whom correspondence should be addressed. ating@mit.edu.

‡Current address: Ulsan National Institute of Science and Technology (UNIST), Ulsan, Korea

The authors have no conflicting financial interests. A patent application has been filed by MIT relating to this work. Proteomic data can be found in Supplementary Tables S1 to S9. The authors will make the genetic constructs used in this work widely available to the academic community through Addgene.

We recently introduced engineered ascorbate peroxidase (APEX) as a genetic tag for electron microscopy (EM) (5). Unlike HRP, APEX is active within all cellular compartments. In addition to catalyzing the H₂O₂-dependent polymerization of diaminobenzidine for EM contrast, APEX also oxidizes numerous phenol derivatives to phenoxyl radicals. Such radicals are short lived (<1 msec (6, 7)) have a small labeling radius (<20 nm (8, 9)) and can covalently react with electron-rich amino acids such as Tyr, Trp, His and Cys (10–13). This chemistry forms the basis of tyramide signal amplification (14) but it has not been extended to living cells.

To examine whether APEX could be employed for proteomic labeling (Fig. 1A), we targeted APEX to the mitochondrial matrix of human embryonic kidney (HEK) cells, and initiated labeling by adding biotin-phenol and 1 mM H₂O₂ to the cell medium. Labeling was terminated after 1 minute by cell fixation or lysis. Imaging by confocal (Fig. 1B) or super-resolution STORM (15) (Fig. 1C) microscopy showed that biotinylated proteins overlapped tightly with the mito-APEX construct. Streptavidin blot analysis of cell lysate showed that numerous endogenous proteins were biotinylated in an APEX- and H₂O₂-dependent manner (Figs. 1D and S3).

Other constructs targeting APEX to different cellular regions were also analyzed to test the generality of the approach (Figs. S4–S5). Seven different cytosol-facing APEX fusions each gave distinct “fingerprints” in a streptavidin blot analysis, suggesting that targeted APEX biotinylates only a subset of cytosolic proteins, likely those in its immediate vicinity. Additional experiments were performed to characterize the small-molecule specificity of APEX (Fig. S2), the membrane permeability of the phenoxyl radical (Fig. S6), and covalent adducts formed with amino acids *in vitro* (Fig. S7).

We used mitochondrial matrix-targeted APEX to perform a proteomic experiment. Though mitochondria have been extensively characterized by MS proteomics, all previous studies have used mitochondrial purification, which is associated with sample loss and contamination. This is why the most comprehensive inventory of mitochondrial proteins (16) integrates MS proteomic data with GFP imaging and computational analysis. Furthermore, proteome-scale maps of the matrix subcompartment in mammalian cells contain only a small number of proteins (17), representing very low coverage, likely because of the challenge of enriching for this subcompartment.

Endogenous proteins biotinylated by mito-APEX for 1 minute in live HEK cells as in Fig. 1 were purified using streptavidin beads, digested to peptides, and identified by tandem MS. We used stable isotope labeling (SILAC (18)) of experimental and control samples to distinguish between biotinylated proteins and non-specific binders (Fig. S8). Two independent replicates were performed and each produced a bimodal distribution of proteins based on isotope ratio (Fig. S8C). The high-ratio distributions were strongly enriched for mitochondrial proteins, so we separated these hits and intersected the results from both replicates to obtain a list of 495 proteins (Table S1), which we call our “matrix proteome.” This list is expected to contain both soluble matrix proteins and inner mitochondrial membrane proteins that are exposed to the matrix space.

Crossing our matrix proteome with prior literature revealed that it was highly enriched for both mitochondrial and mitochondrial matrix proteins (Fig. 2A). 464 proteins (94%) had prior mitochondrial annotation, leaving 31 “mitochondrial orphans” without any previously known connection to mitochondria (Table S2). To further quantify the specificity of our matrix proteome, we examined the components of the electron transport chain (Fig. 2C) and the TOM/TIM/PAM protein import pathway (Fig. 2D), because they are structurally and/or topologically well-characterized. Only subunits with exposure to the matrix space were

detected in our matrix proteome, illustrating the specificity and membrane-impermeability of our tagging.

To analyze depth of coverage, we checked our matrix proteome for well-established groups of soluble matrix proteins (Fig. 2B). 80–90% of the members of each group were detected. Nearly identical subsets of proteins were detected in each of the two replicates, suggesting that coverage was high, but only for ~85% of proteins. The proteins we consistently did not detect were not low-abundance proteins (Fig. S8F), and they did not lack surface-exposed tyrosines. We hypothesize that these proteins were sterically buried in macromolecular complexes, making them inaccessible to the phenoxyl radical.

For a subset of proteins in our proteome, we detected directly biotinylated peptides (Fig. S9 and Table S4). Tandem MS sequencing showed that the biotin-phenol was conjugated to tyrosine sidechains. In nearly all cases, the biotinylated tyrosine mapped to a surface-exposed site on a soluble protein, or a matrix-exposed site on a transmembrane protein.

Our matrix proteome of 495 proteins provides a number of interesting insights. First, the 31 mitochondrial orphans may be newly discovered mitochondrial proteins. We selected and imaged six of these at random and found complete or partial mitochondrial localization for all of them (Fig. S10). Second, 240 proteins with unknown sub-mitochondrial localization can now be assigned by our data to the matrix compartment (Table S3). Third, we detected six proteins previously assigned to the IMS or outer mitochondrial membrane (PPOX, CPOX, PNPT1, CHCHD3, COASY, and SAMM50). To determine if our detection of these proteins in the matrix was accurate, we performed EM imaging, taking advantage of APEX's additional functionality as an EM tag (5). APEX fusions to five of the six proteins showed matrix staining by EM (Figs. 3 and S11). We were unable to examine one protein, SAMM50, because APEX insertion at four different sites abolished mitochondrial targeting (data not shown).

PPOX and CPOX are particularly interesting in this group because they catalyze two of the later steps in heme biosynthesis (Fig. 3A). Previous studies on purified mitochondria or mitoplasts treated with proteases or membrane-impermeant inhibitors have localized both enzymes to the IMS (19–22). Structural analysis and modeling have suggested that PPOX docks to FECH (ferrochelatase), the final iron-inserting enzyme of heme biosynthesis, through the inner mitochondrial membrane (IMM) (23) (Fig. 3F). This model is inconsistent with our EM data because we found that both the C-terminus and amino acid 205 of PPOX localize to the matrix (Fig. 3C). Our EM data on CPOX, on the other hand, are consistent with previous literature, because we found that residue 70 localizes to the matrix (explaining CPOX's detection in our matrix proteome), while the C-terminus and residue 120 flanking the active site localized to the IMS (Fig. 3D). Our reassignment of PPOX from the IMS to the matrix has implications for the nature of its interactions with CPOX and FECH and the mechanism by which its heme precursor substrate is transported across the IMM.

In summary, we have developed a method for mapping the proteomic composition of cellular organelles, using a genetically-targetable peroxidase that catalyzes the generation of short-lived, highly-reactive, and membrane-impermeant radicals in live cells. With a temporal resolution of 1 minute, labeled proteins are harvested and identified by MS using well-established techniques. In addition to its simplicity, the method has no noticeable toxicity, requires far less material than conventional organellar proteomics, and takes hours to implement rather than days (as for subcellular fractionation). Our initial demonstration on the human mitochondrial matrix proteome shows that specificity is exceptionally high, because labeling is performed in living cells while membranes and other structures are still intact. A key feature of the method is that it provides insight into the topology of identified

proteins. Depth of coverage is also high for the majority of proteins – likely those that are sterically accessible to the phenoxyl radical. Finally, the same peroxidase, APEX, can be used for both proteomic mapping and EM visualization (5).

Supplementary Material

Refer to Web version on PubMed Central for supplementary material.

Acknowledgments

We thank N. Watson (Whitehead Institute Keck Microscopy Facility) and E. Vasile (Koch Institute Microscopy Core Facility) for performing EM imaging; H. B. Fraser for assistance with data analysis and manuscript editing; C. Uttamapinant for picoyl azide-AF647; X. Zhuang and her lab for advice on STORM microscopy; H. A. Dailey for advice on CPOX and PPOX; and S. Calvo for assistance with data analysis. Funding was provided by the NIH (DP1 OD003961 to A.Y.T. and R01 GM077465 to V.K.M.), Dreyfus Foundation (A.Y.T.), American Chemical Society (A.Y.T.), and Broad Institute of MIT and Harvard (S.A.C.).

References and Notes

1. Roux KJ, Kim DI, Raida M, Burke B. A promiscuous biotin ligase fusion protein identifies proximal and interacting proteins in mammalian cells. *J. Cell. Biol.* 2012; 196:801. [PubMed: 22412018]
2. Morriswood B, et al. Novel bilobe components in *Trypanosoma brucei* identified using proximity-dependent biotinylation. *Eukaryot. Cell.* 2012
3. Choi-Rhee E, Schulman H, Cronan JE. Promiscuous protein biotinylation by *Escherichia coli* biotin protein ligase. *Protein. Sci.* 2004; 13:3043. [PubMed: 15459338]
4. Kotani N, et al. Biochemi visualization of cell surface molecular clustering in living cells. *Proc. Natl. Acad. Sci. U.S.A.* 2008; 105:7405. [PubMed: 18495923]
5. Martell JD, et al. Engineered ascorbate peroxidase as a genetically encoded reporter for electron microscopy. *Nat. Biotechnol.* 2012; 30:1143. [PubMed: 23086203]
6. Wishart, JF.; Madhava Rao, BS. Recent trends in radiation chemistry. World Scientific; Singapore: 2010. p. 577-596.
7. Mortensen A, Skibsted LH. Importance of carotenoid structure in radical-scavenging reactions. *J. Agr. Food. Chem.* 1997; 45:2970.
8. Bendayan M. Tech.Sight. Worth its weight in gold. *Science.* 2001; 291:1363. [PubMed: 11233453]
9. Mayer G, Bendayan M. Biotinyl-tyramide: a novel approach for electron microscopic immunocytochemistry. *J. Histochem. Cytochem.* 1997; 45:1449. [PubMed: 9358846]
10. Minamihata K, Goto M, Kamiya N. Protein heteroconjugation by the peroxidase-catalyzed tyrosine coupling reaction. *Bioconj. Chem.* 2011; 22:2332. [PubMed: 21999311]
11. Rogers MS, et al. Cross-link formation of the cysteine 228-tyrosine 272 catalytic cofactor of galactose oxidase does not require dioxygen. *Biochemistry.* 2008; 47:10428. [PubMed: 18771294]
12. Bhaskar B, et al. A novel heme and peroxide-dependent tryptophan-tyrosine cross-link in a mutant of cytochrome c peroxidase. *J. Mol. Biol.* 2003; 328:157. [PubMed: 12684005]
13. Amini F, Kodadek T, Brown KC. Protein affinity labeling mediated by genetically encoded peptide tags. *Angew. Chem. Int. Ed. Engl.* 2002; 41:356. [PubMed: 12491432]
14. Schonhuber W, Fuchs B, Juretschko S, Amann R. Improved sensitivity of whole-cell hybridization by the combination of horseradish peroxidase-labeled oligonucleotides and tyramide signal amplification. *Appl. Environ. Microbiol.* 1997; 63:3268. [PubMed: 9251215]
15. Huang B, Bates M, Zhuang XW. Super-Resolution Fluorescence Microscopy. *Annu. Rev. Biochem.* 2009; 78:993. [PubMed: 19489737]
16. Pagliarini DJ, et al. A mitochondrial protein compendium elucidates complex I disease biology. *Cell.* 2008; 134:112. [PubMed: 18614015]

17. Forner F, Foster LJ, Campanaro S, Valle G, Mann M. Quantitative proteomic comparison of rat mitochondria from muscle, heart, and liver. *Mol. Cell. Proteomics*. 2006; 5:608. [PubMed: 16415296]
18. Ong SE, et al. Stable isotope labeling by amino acids in cell culture, SILAC, as a simple and accurate approach to expression proteomics. *Mol. Cell. Proteomics*. 2002; 1:376. [PubMed: 12118079]
19. Ferreira GC, Andrew TL, Karr SW, Dailey HA. Organization of the terminal two enzymes of the heme biosynthetic pathway. Orientation of protoporphyrinogen oxidase and evidence for a membrane complex. *J. Biol. Chem.* 1988; 263:3835. [PubMed: 3346226]
20. Deybach JC, da Silva V, Grandchamp B, Nordmann Y. The mitochondrial location of protoporphyrinogen oxidase. *Eur. J. Biochem.* 1985; 149:431. [PubMed: 3996415]
21. Elder GH, Evans JO. Evidence that the coproporphyrinogen oxidase activity of rat liver is situated in the intermembrane space of mitochondria. *Biochem. J.* 1978; 172:345. [PubMed: 666752]
22. Grandchamp B, Phung N, Nordmann Y. The mitochondrial localization of coproporphyrinogen III oxidase. *Biochem. J.* 1978; 176:97. [PubMed: 31872]
23. Koch M, et al. Crystal structure of protoporphyrinogen IX oxidase: a key enzyme in haem and chlorophyll biosynthesis. *EMBO J.* 2004; 23:1720. [PubMed: 15057273]
24. Hamza I, Dailey HA. One ring to rule them all: Trafficking of heme and heme synthesis intermediates in the metazoans. *Bba-Mol. Cell. Res.* 2012; 1823:1617.
25. Nilsson R, et al. Discovery of genes essential for heme biosynthesis through large-scale gene expression analysis. *Cell. Metab.* 2009; 10:119. [PubMed: 19656490]
26. Qin X, et al. Structural insight into human variegate porphyria disease. *FASEB J.* 2011; 25:653. [PubMed: 21048046]

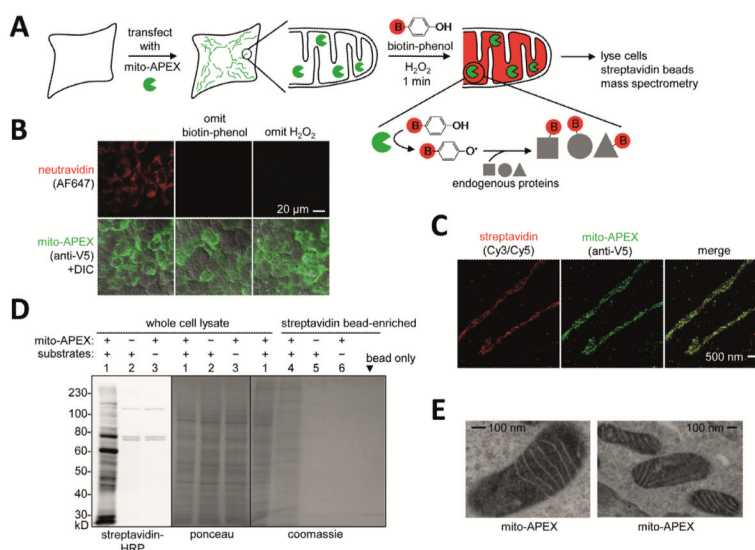


Fig. 1. Labeling the mitochondrial matrix proteome in living HEK cells

(A) Labeling scheme. The APEX peroxidase was genetically targeted to the mitochondrial matrix via fusion to a 24-amino acid targeting peptide (5). Labeling was initiated by addition of biotin-phenol and H_2O_2 to live cells for 1 minute. Cells were then lysed, and biotinylated proteins recovered with streptavidin-coated beads, eluted, separated on a gel, and identified by mass spectrometry. The peroxidase-generated phenoxyl radical is short-lived and membrane-impermeant and hence covalently tags only neighboring and not distant endogenous proteins. (B) Confocal fluorescence imaging of biotinylated proteins (stained with neutravidin), after live labeling of HEK cells expressing mito-APEX as in (A). Controls were performed with either biotin-phenol or H_2O_2 omitted. (C) Super-resolution STORM images showing streptavidin and APEX (AF405/AF647) localization patterns at 22 nm resolution in U2OS cells. Samples were reacted as in (B). (D) Gel analysis of biotinylated mitochondrial matrix proteins, before (lanes 1–3) and after (lanes 4–6) streptavidin bead-enrichment. Samples were labeled as in (B). Substrates are biotinphenol and H_2O_2 . Mammalian cells have four endogenously biotinylated proteins, three of which were observed in the negative control lanes (2–3) of the streptavidin blot. (E) Electron microscopy (EM) of HEK cells expressing mito-APEX. EM contrast was generated by treating fixed cells with H_2O_2 and diaminobenzidine. APEX catalyzes the polymerization of diaminobenzidine into a local precipitate, which is subsequently stained with electron-dense OsO_4 (5). Dark contrast is apparent in the mitochondrial matrix, but not the intermembrane space.

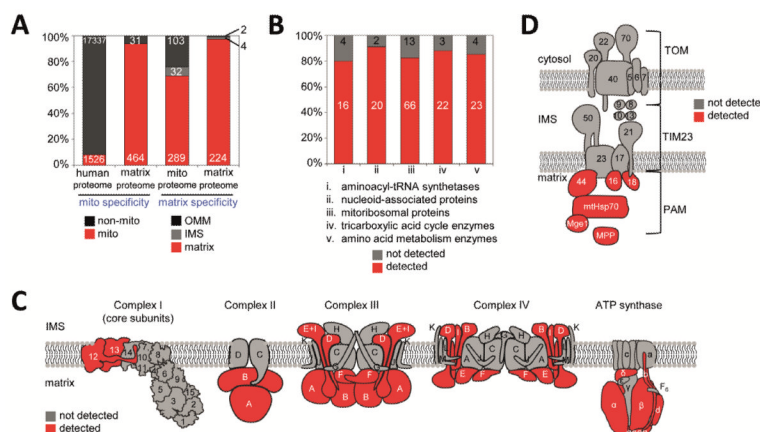


Fig. 2. Specificity and depth of coverage of the mitochondrial matrix proteome

(A) Analysis of specificity. Left two columns show the fraction of proteins with prior mitochondrial annotation in the entire human proteome (column 1) and in our matrix proteome (column 2). Right two columns show the distribution of proteins with prior sub-mitochondrial localization information, for all mitochondrial proteins (column 3), and for our matrix proteome (column 4). See Table S6 for details. (B) Analysis of depth of coverage. Five groups of well-established mitochondrial matrix proteins (i–v) were crossed with our proteomic list. For each group, 80–91% of proteins were detected in our matrix proteome. See Table S7 for details. (C) Analysis of labeling specificity for protein complexes of the inner mitochondrial membrane. The subunits of Complexes I–IV and F₀–F₁ ATP synthase, for which structural information is available, are illustrated. Subunits detected in our proteome are shaded red; those not detected are shaded grey. Note that because structural information is not available for all 45 subunits of Complex I, some subunits that appear exposed here may not be exposed in the complete complex. (D) Same analysis as in (C), for proteins of the TOM/TIM/PAM protein import machinery that spans the outer and inner mitochondrial membranes. All proteins depicted in (C) and (D) are listed, with additional information, in Table S8.

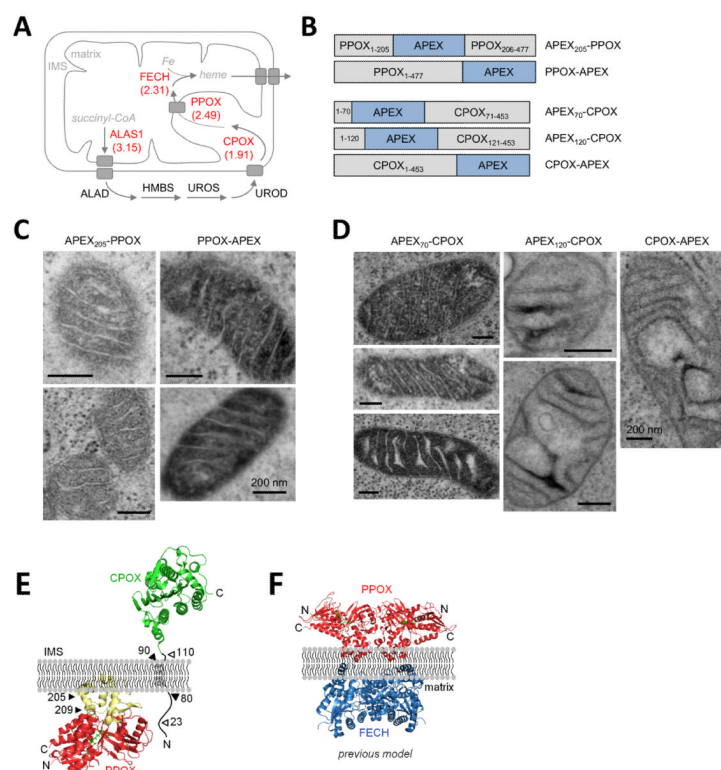


Fig. 3. Sub-mitochondrial localization of the heme biosynthesis enzymes CPOX and PPOX
(A) Model showing the sub-mitochondrial localizations of the eight core enzymes that catalyze heme biosynthesis, according to previous literature (24). Four of these enzymes are detected in our matrix proteome and are colored red (with $\log_2(H/L)$ ratios from replicate 1 shown). Drawing adapted from (25). **(B)** Domain structures of PPOX and CPOX fusions to APEX, imaged by EM in **(C)** and **(D)**, respectively. Additional EM images of PPOX-APEX are shown in Fig. S11B. **(E)** Our model for PPOX and CPOX localization, based on our EM data and previous literature (19–22). The predicted membrane-binding region of PPOX (residues 92–209) is colored yellow (26). Hollow arrowheads point to predicted cleavage sites in CPOX. **(F)** Previous model showing the docking of a PPOX dimer and a FECH (ferrochelatase) dimer through the inner mitochondrial membrane (23). N- and C-terminal ends of PPOX are labeled. Our data contradict this model because the EM images in **(C)** show that the C-terminus and residue 205 of PPOX are in the matrix, not the IMS.